Hindawi Publishing Corporation
Advances in Mathematical Physics
Volume 2012, Article ID 657805, 13 pages
doi:10.1155/2012/657805

Research Article

Heat Transfer in MHD Dusty Boundary Layer Flow over an Inclined Stretching Sheet with Non-Uniform Heat Source/Sink

G. K. Ramesh, B. J. Gireesha, and C. S. Bagewadi

Department of Studies and Research in Mathematics, Kuvempu University, Shankaraghatta, Shimoga, Karnataka 577 451, India

Correspondence should be addressed to B. J. Gireesha, bjgireesu@rediffmail.com

Received 1 March 2012; Revised 28 April 2012; Accepted 30 April 2012

Academic Editor: Shao-Ming Fei

This paper presents the study of momentum and heat transfer characteristics in a hydromagnetic flow of dusty fluid over an inclined stretching sheet with non-uniform heat source/sink, where the flow is generated due to a linear stretching of the sheet. Using a similarity transformation, the governing equations of the problem are reduced to a coupled third-order nonlinear ordinary differential equations and are solved numerically by Runge-Kutta-Fehlberg fourth-fifth-order method using symbolic software Maple. Our numerical solutions are shown to agree with the available results in the literature and then employ the numerical results to bring out the effects of the fluid-particle interaction parameter, local Grashof number, angle of inclination, heat source/sink parameter, Chandrasekhar number, and the Prandtl number on the flow and heat transfer characteristics. The results have possible technological applications in liquid-based systems involving stretchable materials.

1. Introduction

Investigations of boundary layer flow and heat transfer are important due to its applications in industries, and many manufacturing processes such as aerodynamic extrusion of plastic sheets, cooling of metallic sheets in a cooling bath, which would be in the form of an electrolyte, and polymer sheet extruded continuously from a die are few practical applications of moving surfaces. Glass blowing, continuous casting, and spinning of fibers also involve the flow due to stretching surface. During its manufacturing process, a stretched sheet interacts with the ambient fluid thermally and mechanically. The thermal interaction is governed by the surface heat flux. This surface heat flux can either be prescribed, or it is the output of a process in which the surface temperature distribution has been prescribed.

Newton's law of viscosity states that shear stress is proportional to velocity gradient. Thus, the fluids that obey this law are known as Newtonian fluids.

Crane [3] investigated the flow due to a stretching sheet with linear surface velocity and obtained the similarity solution to the problem. Later, this problem has been extended to various aspects by considering non-Newtonian fluids, more general stretching velocity, magnetohydrodynamic (MHD) effects, porous sheets, porous media, and heat or mass transfer. Andresson et al. [4] extended the work of Crane [3] to non-Newtonian power law fluid over a linear stretching sheet. Grubka and Bobba [5] analyzed heat transfer studies by considering the power-law variation of surface temperature. Saffman [6] has discussed the stability of the laminar flow of a dusty gas in which the dust particles are uniformly distributed. Chakrabarti [7] analyzed the boundary layer flow of a dusty gas. Datta and Mishra [8] have investigated dusty fluid in boundary layer flow over a semi-infinite flat plate. Further, Xie et al. [9] have extended the work of [8] and studied on the hydrodynamic stability of a particle-laden flow in growing flat plate boundary layer. Palani and Ganesan [10] have studied heat transfer effects on dusty gas flow past a semi-infinite inclined plate; in this paper, they have nondimensionalised the governing boundary layer equations. Agranat [11] has discussed the effect of pressure gradient on friction and heat transfer in a dusty boundary layer. Chakrabarti and Gupta [12] have studied the hydromagnetic flow and heat transfer in a fluid initially at rest and at uniform temperature over a stretching sheet at a different uniform temperature. Vajravelu and Nayfeh [13] analyzed the hydromagnetic flow of dusty fluid over a stretching sheet with the effect of suction. Further, Vajravelu and Roper [1] studied the flow and heat transfer in a second-grade fluid over a stretching sheet with viscous dissipation and internal heat generation or absorption. Tsai et al. [2] extended the work of [1] and studied an unsteady flow over a stretching surface with non-uniform heat source. Cortell [14] studied the magnetohydrodynamics flow of a power-law fluid over a stretching sheet. Abel and Mahesha [15] presented an analytical and numerical solution for heat transfer in a steady laminar flow of an incompressible viscoelastic fluid over a stretching sheet with power-law surface temperature, including the effects of variable thermal conductivity and non-uniform heat source and radiation. Chen [16] studied Magnetohydrodynamic mixed convection of a power-law fluid past a stretching surface in the presence of thermal radiation and internal heat generation/absorption. Gireesha et al. [17] studied boundary layer flow and heat transfer of a dusty fluid flow over a stretching sheet with non-uniform heat source/sink. Samad and Mohebujjaman [18] investigated the case along a vertical stretching sheet in the presence of magnetic field and heat generation.

Since the study of heat source/sink effect on heat transfer is important in some cases, in the present paper, we studied the hydromagnetic flow and heat transfer of a dusty fluid over an inclined stretching sheet with the effect of non-uniform heat source/sink. The resulting governing equations are transformed into a system of nonlinear ordinary differential equations by applying a suitable similarity transformation. These equations are solved numerically by RKF 45 using Maple and discussed the results from the physical point of view.

2. Flow Analysis of the Problem

Consider two-dimensional steady laminar boundary layer flow of an incompressible viscous dusty fluid over a vertical stretching sheet which is inclined with an acute angle α and situated in the fluid of ambient temperature T_∞. The x-axis moves along the stretching surface

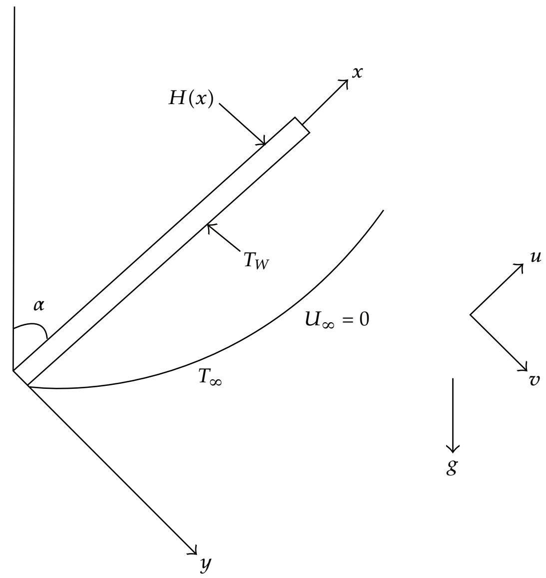

Figure 1: Geometrical configuration of the flow problem.

in the direction of motion with the slot as the origin, and the y-axis is measured normally from the sheet to the fluid. Further, the flow field is exposed to the influence of an external transverse magnetic field of strength H_0 (along y-axis) as shown in Figure 1. Both the fluid and dust particle clouds are supposed to be static at the beginning. The dust particles are assumed to be spherical in shape and uniform in size, and number density of the dust particle is taken as a constant throughout the flow.

Under the above assumption and along with Boussinesq's approximation, the basic two-dimensional boundary layer equations are as follows [13]:

$$\frac{\partial u}{\partial x} + \frac{\partial v}{\partial y} = 0, \tag{2.1}$$

$$u\frac{\partial u}{\partial x} + v\frac{\partial u}{\partial y} = \frac{\mu}{\rho}\frac{\partial^2 u}{\partial y^2} + \frac{KN}{\rho}(u_p - u) + g\beta^*(T - T_\infty)\cos\alpha - \frac{\sigma H_0^2 u}{\rho}, \tag{2.2}$$

$$u_p\frac{\partial u_p}{\partial x} + v_p\frac{\partial u_p}{\partial y} = \frac{K}{m}(u - u_p), \tag{2.3}$$

$$u_p\frac{\partial v_p}{\partial x} + v_p\frac{\partial v_p}{\partial y} = \frac{K}{m}(v - v_p), \tag{2.4}$$

$$\frac{\partial}{\partial x}(\rho_p u_p) + \frac{\partial}{\partial y}(\rho_p v_p) = 0, \tag{2.5}$$

where (u, v) and (u_p, v_p) are the velocity components of the fluid and dust particle phases along x and y directions, respectively. μ, ρ, ρ_p, and N are the coefficient of viscosity of the fluid, density of the fluid, density of the dust particle, and number density of the particle phase, respectively, H_0 is the strength of applied magnetic field, K is the stokes' resistance (drag coefficient), T and T_∞ are the fluid temperature within the boundary layer and in the free stream, respectively, g is the acceleration due to gravity, β^* is the volumetric coefficient of thermal expansion, and m is the mass of the dust particle. It is also assumed that the external electric field is zero, and the electric field due to polarization of charges is negligible. In deriving these equations, the drag force is considered for the interaction between the fluid and dust phases.

The boundary conditions for the flow problem are given by

$$\begin{gathered} u = U_w(x), \quad v = 0, \quad \text{at } y = 0, \\ u \longrightarrow 0, \quad u_p \longrightarrow 0, \quad v_p \longrightarrow v, \quad \rho_p \longrightarrow \omega\rho, \quad \text{as } y \longrightarrow \infty, \end{gathered} \tag{2.6}$$

where $U_w(x) = cx$ is the stretching sheet velocity, $c > 0$; this is known as stretching rate, and ω is the density ratio.

To convert the governing equations into a set of similarity equations, we introduce the following transformation:

$$\begin{gathered} u = cxf'(\eta), \qquad v = -\sqrt{\nu c}\, f(\eta), \qquad \eta = \sqrt{\frac{c}{\nu}}y, \\ u_p = cxF(\eta), \qquad v_p = \sqrt{\nu c}G(\eta), \qquad \rho_r = H(\eta), \end{gathered} \tag{2.7}$$

which identically satisfy (2.1), and substituting (2.7) into (2.2)–(2.5), one can obtain the following nonlinear ordinary differential equations:

$$f''' + ff'' - (f')^2 + l^*\beta H\ [F - f'] + \mathrm{Gr}\,\theta\cos\alpha - Qf' = 0, \tag{2.8}$$

$$GF' + F^2 + \beta[F - f'] = 0, \tag{2.9}$$

$$GG' + \beta[f + G] = 0, \tag{2.10}$$

$$HF + HG' + GH' = 0, \tag{2.11}$$

where a prime denotes differentiation with respect to η and $l^* = mN/\rho$, $\tau = m/K$ is the relaxation time of the particle phase, $\beta = 1/c\tau$ is the fluid particle interaction parameter, $\mathrm{Gr} = (g\beta^*(T_w - T_\infty))/c^2x$ is the local Grashof number (Kierkus [19]), $Q = \sigma H_0^2/c\rho$ is the Chandrasekhar number, and $\rho_r = \rho_p/\rho$ is the relative density.

The boundary conditions defined as in (2.6) will become,

$$\begin{gathered} f = 0, \quad f' = 1, \quad \text{at } \eta = 0, \\ f' = 0, \quad F = 0, \quad G = -f, \quad H = \omega, \quad \text{as } \eta \longrightarrow \infty. \end{gathered} \tag{2.12}$$

If $\beta = 0$, $\mathrm{Gr} = 0$, the analytical solution of (2.8) with boundary condition (2.12) can be written

Table 1: Comparison of $\theta'(0)$ for various values of Pr and B^* when $\beta = 0$, Gr = 0, $A^* = 0$, $Q = 0$, Ec = 0, and $N = 0$.

B^*	Pr	Vajravelu and Roper [1]	Tsai et al. [2]	Present Study $\theta'(0)$
−2	2	−2.4860	−2.4859	−2.4859
−3	3	−3.0281	−3.0281	−3.0281
−4	4	−3.5851	−3.5851	−3.5851

Table 2: Comparison of $-f''(0)$ for various values of Q when $\beta = 0$, Gr = 0, $A^* = 0$, $B^* = 0$, Ec = 0, and Pr = 0.

Q	Cortell [14]	Chen [16]	Present study $-f''(0)$
0.0	1.000	1.000	1.001
0.2	1.095	1.095	1.095
0.5	1.224	1.224	1.224
1.0	1.414	1.414	1.414
1.2	1.483	1.483	1.483
1.5	1.581	1.581	1.581
2.0	1.732	1.732	1.732

in the form of

$$f = \frac{1 - e^{-\xi\,\eta}}{\xi}, \tag{2.13}$$

where $\xi = \sqrt{Q+1}$.

3. Heat Transfer Analysis

The governing boundary layer heat transport equations for a dusty fluid in the presence of non-uniform internal heat source/sink for two-dimensional flows are given by [17]

$$\begin{gathered} \rho c_p\left(u\frac{\partial T}{\partial x} + v\frac{\partial T}{\partial y}\right) = k\frac{\partial^2 T}{\partial y^2} + \frac{N c_p}{\tau_T}\left(T_p - T\right) + \frac{N}{\tau_v}\left(u_p - u\right)^2 + q''', \\ u_p\frac{\partial T_p}{\partial x} + v_p\frac{\partial T_p}{\partial y} = -\frac{c_p}{c_m}\left(T_p - T\right), \end{gathered} \tag{3.1}$$

where T and T_p are the temperature of the fluid and temperature of the dust particle, respectively, c_p and c_m are the specific heat of fluid and dust particles, τ_T is the thermal equilibrium time, that is, the time required by the dust cloud to adjust its temperature to the fluid, τ_v is the relaxation time of the dust particle, that is, the time required by a dust particle to adjust its velocity relative to the fluid, and k is the thermal conductivity. q''' is the space- and temperature-dependent internal heat generation/absorption (non-uniform heat source/sink) which can be expressed as

$$q''' = \left(\frac{kU_w(x)}{x\nu}\right)\left[A^*\left(T_w - T_\infty\right)f' + B^*\left(T - T_\infty\right)\right], \tag{3.2}$$

where T_w and T_∞ denote the temperature at the wall and at large distance from the wall,

Table 3: Values of wall velocity gradient $-f''(0)$ temperature gradient $-\theta'(0)$ for different values of β, α, Q, Gr, A^*, B^*, Pr, and Ec.

β	Ec	Pr	Gr	α	A^*	B^*	Q	$-\theta'(0)$	$-f''(0)$
0.2	2.0	1.0	0.5	30°	0.5	0.5	3.0	−0.29336	1.96310
0.5								0.32170	1.98318
0.9								0.48237	1.99059
0.5	0.0	1.0	0.5	30°	0.5	0.5	3.0	0.71588	1.98532
	1.0							0.51878	1.98425
	2.0							0.32170	1.98318
0.5	2.0	1.0	0.5	30°	0.5	0.5	3.0	0.32170	1.98318
		2.0						1.19511	1.99348
		3.0						1.66299	1.99689
0.5	2.0	1.0	0.0	30°	0.5	0.5	3.0	0.23283	2.01714
			0.5					0.32170	1.98318
			1.0					0.37466	1.95115
0.5	2.0	1.0	0.5	0°	0.5	0.5	3.0	1.01930	1.85135
				30°				0.98397	1.99098
				90°				0.94359	2.09512
0.5	2.0	1.0	0.5	30°	−0.5	0.5	3.0	0.79070	1.98753
					0.0			0.55715	1.98537
					0.5			0.32170	1.98318
0.5	2.0	1.0	0.5	30°	0.5	−0.5	3.0	1.12197	1.99266
						0.0		0.85246	1.99013
						0.5		0.32170	1.98318
0.5	2.0	1.0	0.5	30°	0.5	0.5	1.0	0.53643	1.39971
							2.0	0.44219	1.71607
							3.0	0.32170	1.98318

respectively. A^* and B^* are the parameters of the space- and temperature-dependent internal heat source/sink. It is to be noted that A^* and B^* are positive to internal heat source and negative to internal heat sink; ν is the kinematic viscosity.

In order to solve the (3.1), the nondimensional temperature boundary conditions are defined in a quadratic form as

$$\begin{aligned} &T = T_w = T_\infty + A\left(\frac{x}{l}\right)^2, \quad \text{at } y = 0, \\ &T \longrightarrow \infty, \quad T_p \longrightarrow T_\infty, \quad \text{as } y \longrightarrow \infty, \end{aligned} \tag{3.3}$$

where T_w and T_∞ denote the temperature at the wall and at large distance from the wall, respectively, A is a positive constant, and $l = \sqrt{\nu/c}$ is a characteristic length.

Now, we define the nondimensional fluid-phase temperature $\theta(\eta)$ and dust-phase temperature $\theta_p(\eta)$ as

$$\theta(\eta) = \frac{T - T_\infty}{T_w - T_\infty}, \qquad \theta_p(\eta) = \frac{T_p - T_\infty}{T_w - T_\infty}, \tag{3.4}$$

where $T - T_\infty = A(x/l)^2\theta(\eta)$.

Using (3.4) into (3.1), we get the following non-linear ordinary differential equations:

$$\theta'' + \Pr\left[f\theta' - 2f'\theta\right] + \frac{N\Pr}{\rho c\tau_T}\left[\theta_p - \theta\right] + \frac{N\Pr\mathrm{Ec}}{\rho\tau_v}\left[F - f'\right]^2 + A^* f' + B^*\theta = 0, \tag{3.5}$$

$$2F\theta_p + G\theta_p' + \frac{c_p}{cc_m\tau_T}\left(\theta_p - \theta\right) = 0, \tag{3.6}$$

where $\Pr = \mu c_p/k$ is the Prandtl number, and $\mathrm{Ec} = cl^2/Ac_p$ is the Eckert number.

The corresponding boundary conditions for θ and θ_p are

$$\begin{gathered}\theta = 1, \quad \text{at } \eta = 0, \\ \theta \longrightarrow 0, \quad \theta_p \longrightarrow 0, \quad \text{as } \eta \longrightarrow \infty.\end{gathered} \tag{3.7}$$

The physical quantities of interest are the skin friction coefficient C_f and the local Nusselt number Nu_x which are defined as

$$C_f = \frac{\tau_w}{\rho U_w^2}, \qquad Nu_x = \frac{xq_w}{k(T_w - T_\infty)}, \tag{3.8}$$

where the surface shear stress τ_w and the surface heat flux q_w are given by

$$\tau_w = \mu\left(\frac{\partial u}{\partial y}\right)_{y=0}, \qquad q_w = -k\left(\frac{\partial T}{\partial y}\right)_{y=0}. \tag{3.9}$$

Using the nondimensional variables, we obtain

$$C_f \mathrm{Re}_x^{1/2} = f''(0), \qquad \frac{Nu_x}{\mathrm{Re}_x^{1/2}} = -\theta'(0). \tag{3.10}$$

4. Results and Discussion

The transformed (2.8) to (2.11) and (3.5) to (3.6) subjected to boundary conditions (2.12) and (3.7) were solved numerically using RKF45 methods with the help of symbolic algebra software Maple, using a procedure used by Aziz [20]. It is very efficient in using the well-known Runge-Kutta-Fehlberg fourth-fifth-order method (RKF45 method) to obtain the numerical solutions of a boundary value problem. The RKF45 algorithm in Maple has been well tested for its accuracy and robustness. In order to validate the numerical results obtained, we compare our results with those reported by Vajravelu and Roper [1] and Tsai et al. [2] for various values of Prandtl number and Cortell [14] and Chen [16] for various values of Q as shown in Tables 1 and 2, and they are found to be in a favorable agreement. The results of velocity gradient $f''(0)$ and temperature gradient function $-\theta'(0)$ at the wall are examined for the values of the parameters which are tabulated in Table 3.

Figure 2 depicts the variation in the velocity profiles for different values of fluid particle interaction parameter β. This figure indicates that as fluid-particle interaction

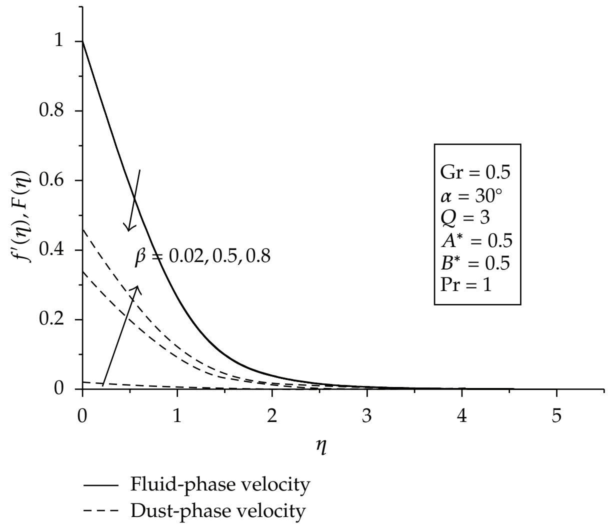

Figure 2: Velocity profile for different values of fluid-particle interaction parameter.

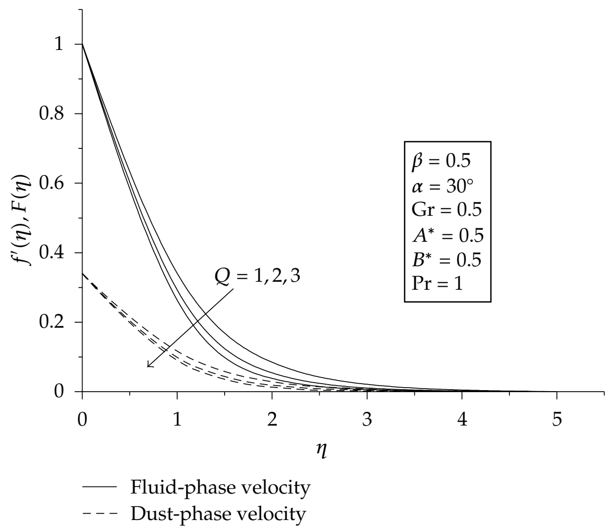

Figure 3: Velocity profile for different values of Chandrasekhar number.

parameter increases, we can see that fluid phase velocity decreases and dust phase velocity increases. Further observation shows that if the dust is very fine, that is, mass of the dust particles is negligibly small, then the relaxation time of dust particle decreases, and ultimately as $\tau \to 0$, the velocities of fluid and dust particles will be the same.

The variation of velocity profiles for various values of the Chandrasekhar number Q is plotted in Figure 3. It is found that the increase in the value of Q is to decrease the velocity profile in the boundary layer. This is due to the fact that the presence of a magnetic field normal to the flow in an electrically conducting fluid produces a Lorentz force, which acts against the flow.

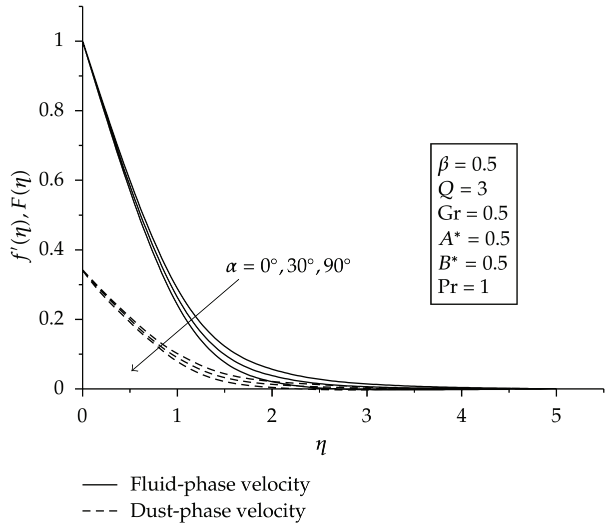

Figure 4: Velocity profile for different values of angle of inclination.

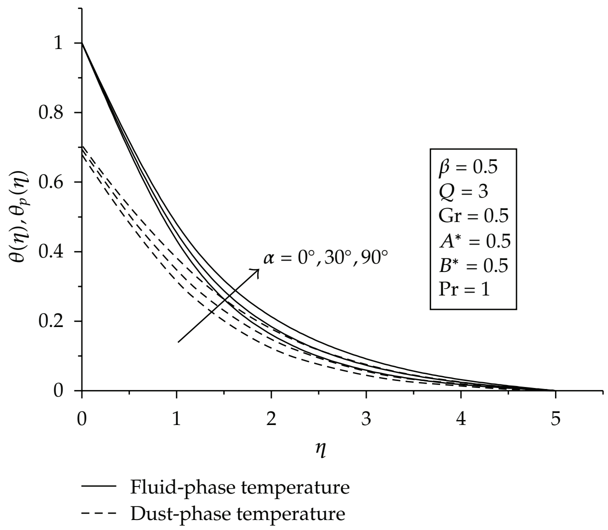

Figure 5: Temperature profile for different values of angle of inclination.

The graph of velocity profiles for typical angles of inclination ($\alpha = 0°, 30°, 90°$) versus η is plotted in Figure 4. It is noted that the angle of inclination increases, and the velocities of fluid and dust phase decrease. This is the fact that the angle of inclination increases the effect of the buoyancy force due to thermal decrease by a factor of $\cos\alpha$. From this figure, it is also noticed that the effect of buoyancy force (which is maximum for $\alpha = 0$) overshoots the main stream velocity significantly. It is also observed that the fluid-phase temperature and dust-phase temperature increase as the angle of inclination increases which are shown in Figure 5.

The graph of local Grashof number Gr on the velocity field is shown in Figure 6. From this plot, it is observed that the effect of increasing values of local Grashof number is to

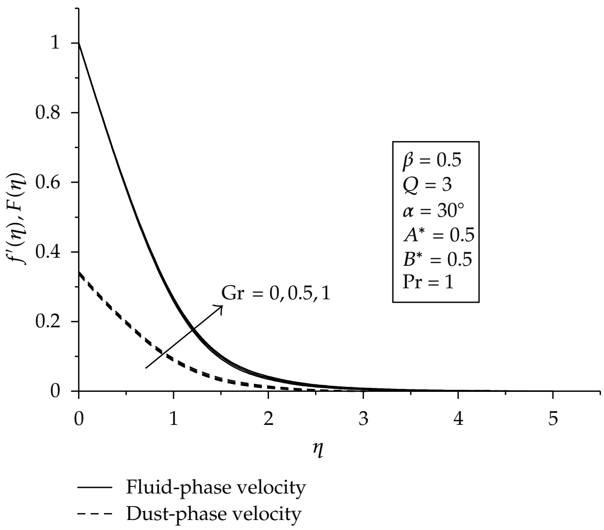

Figure 6: Velocity profile for different values of local Grashof number.

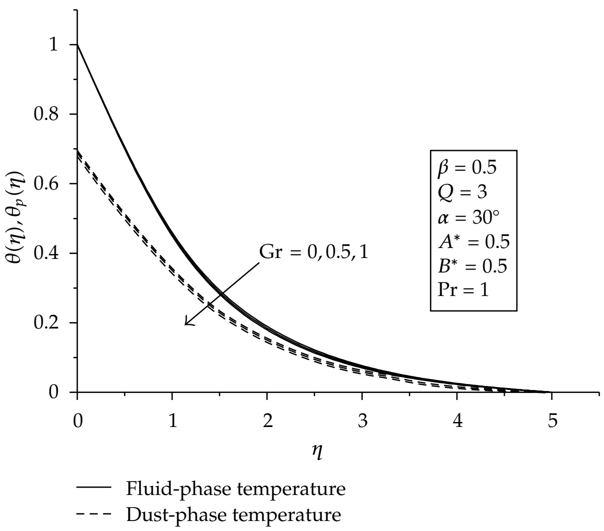

Figure 7: Temperature profile for different values of local Grashof number.

increase the velocity distribution of both the fluid and dust phases. Physically saying that if Gr is positive, it means heating of the fluid or cooling of the boundary surface, and if Gr is negative, it means cooling of the fluid or heating of the boundary surface, and in the absence of Gr, it corresponds to the absence of free convection current. It is evident from Figure 7 that increasing values of Gr decreases the fluid- and dust-phase temperature; this result shows the thinning of the thermal boundary layer.

Figure 8 presents the temperature profiles for different values of space-dependent heat source/sink parameter A^*. It is observed from this figure that the fluid- and dust-phase temperature in the thermal boundary layer increase with the increase in A^*. It can be seen that the thermal boundary layer generates the energy, and the heat sink leads to decrease in

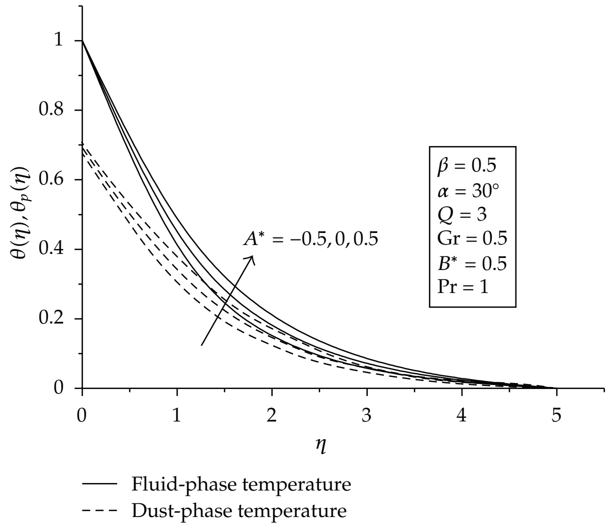

Figure 8: Temperature profile for different values of space-dependent heat source/sink.

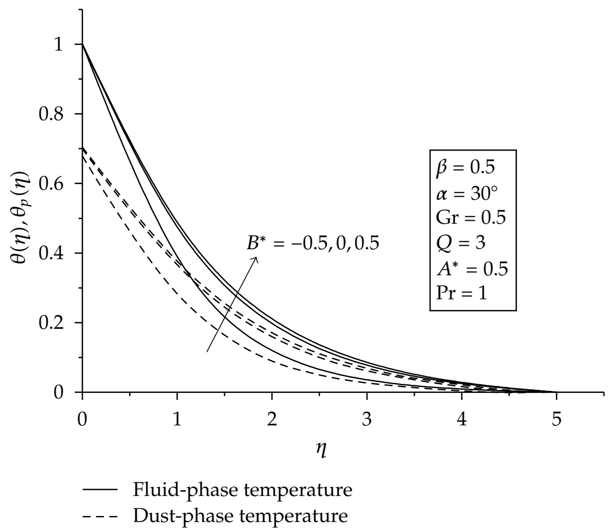

Figure 9: Temperature profile for different values of temperature-dependent heat source/sink.

the thermal boundary layer, whereas the boundary layer thickness increases with increase in A^*. The explanation on the effect of B^* is similar to that given for A^*, and the graph is shown in Figure 9.

The effect of Prandtl number Pr on both fluid- and dust-phase temperature distributions is displayed in Figure 10. It can be seen that the fluid-phase temperature and dust-phase temperature decrease with increase of Prandtl number, which implies momentum boundary layer is thicker than the thermal boundary layer. This is due to the fact that for higher Prandtl number, fluid has a relatively low thermal conductivity, which reduces conduction. From Figures 2 to 10, we can observe that fluid phase is higher than the dust phase, and also it indicates that the fluid phase is parallel to that of dust phase.

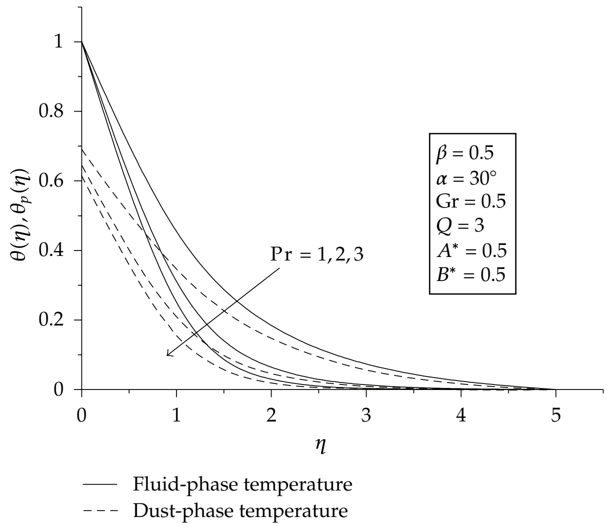

Figure 10: Temperature profile for different values of Prandtl number.

5. Conclusions

In this paper, we have investigated the steady boundary flow and heat transfer of a dusty over an inclined stretching sheet with heat source/sink. Numerical solutions are obtained through Maple. It is very interesting to note that when β increases, clean fluid velocity decreases and dust-fluid velocity increases, and also it is found that the velocity profile decreases as Q and α increase. The thermal boundary layer thickness decreases with increasing Gr and Pr, but increases with increasing α, A^*, and B^*. The values of $\theta'(0)$ increase with the increase Q, Ec, A^*, and B^*; however, they decrease with the increase of β, Gr, and Pr, whereas the values of $f''(0)$ increase with the increase of Gr, Ec, A^*, and B^* and decrease with the increase of β, α, Q, and Pr.

Acknowledgments

The authors are very much thankful to the editor and referee for their encouraging comments and constructive suggestions to improve the presentation of this paper.

References

[1] K. Vajravelu and T. Roper, "Flow and heat transfer in a second grade fluid over a stretching sheet," *International Journal of Non-Linear Mechanics*, vol. 34, no. 6, pp. 1031–1036, 1999.

[2] R. Tsai, K. H. Huang, and J. S. Huang, "Flow and heat transfer over an unsteady stretching surface with non-uniform heat source," *International Communications in Heat and Mass Transfer*, vol. 35, no. 10, pp. 1340–1343, 2008.

[3] L. J. Crane, "Flow past a stretching plate," *Zeitschrift für Angewandte Mathematik und Physik ZAMP*, vol. 21, no. 4, pp. 645–647, 1970.

[4] H. I. Andersson, K. H. Bech, and B. S. Dandapat, "Magnetohydrodynamic flow of a power-law fluid over a stretching sheet," *International Journal of Non-Linear Mechanics*, vol. 27, no. 6, pp. 929–936, 1992.

[5] L. J. Grubka and K. M. Bobba, "Heat transfer characteristics of a continuous stretching surface with variable temperature," *Journal of Heat Transfer*, vol. 107, no. 1, pp. 248–250, 1985.

[6] P. G. Saffman, "On the stability of laminar flow of a dusty gas," *Journal of Fluid Mechanics*, vol. 13, pp. 120–128, 1962.
[7] K. M. Chakrabarti, "Note on Boundary layer in a dusty gas," *AIAA Journal*, vol. 12, no. 8, pp. 1136–1137, 1974.
[8] N. Datta and S. K. Mishra, "Boundary layer flow of a dusty fluid over a semi-infinite flat plate," *Acta Mechanica*, vol. 42, no. 1-2, pp. 71–83, 1982.
[9] M. L. Xie, J. Z. Lin, and F. T. Xing, "On the hydrodynamic stability of a particle-laden flow in growing flat plate boundary layer," *Journal of Zhejiang University: Science A*, vol. 8, no. 2, pp. 275–284, 2007.
[10] G. Palani and P. Ganesan, "Heat transfer effects on dusty gas flow past a semi-infinite inclined plate," *Forschung im Ingenieurwesen/Engineering Research*, vol. 71, no. 3-4, pp. 223–230, 2007.
[11] V. M. Agranat, "Effect of pressure gradient on friction and heat transfer in a dusty boundary layer," *Fluid Dynamics*, vol. 23, no. 5, pp. 730–732, 1989.
[12] A. Chakrabarti and A. S. Gupta, "Hydromagnetic flow and heat transfer over a stretching sheet," *Quarterly of Applied Mathematics*, vol. 37, no. 1, pp. 73–78, 1979.
[13] K. Vajravelu and J. Nayfeh, "Hydromagnetic flow of a dusty fluid over a stretching sheet," *International Journal of Non-Linear Mechanics*, vol. 27, no. 6, pp. 937–945, 1992.
[14] R. Cortell, "A note on magnetohydrodynamic flow of a power-law fluid over a stretching sheet," *Applied Mathematics and Computation*, vol. 168, no. 1, pp. 557–566, 2005.
[15] M. S. Abel and N. Mahesha, "Heat transfer in MHD viscoelastic fluid flow over a stretching sheet with variable thermal conductivity, non-uniform heat source and radiation," *Applied Mathematical Modelling*, vol. 32, no. 10, pp. 1965–1983, 2008.
[16] C. H. Chen, "Magneto-hydrodynamic mixed convection of a power-law fluid past a stretching surface in the presence of thermal radiation and internal heat generation/absorption," *International Journal of Non-Linear Mechanics*, vol. 44, no. 6, pp. 596–603, 2009.
[17] B. J. Gireesha, G. K. Ramesh, M. Subhas Abel, and C. S. Bagewadi, "Boundary layer flow and heat transfer of a dusty fluid flow over a stretching sheet with non-uniform heat source/sink," *International Journal of Multiphase Flow*, vol. 37, no. 8, pp. 977–982, 2011.
[18] M. A. Samad and M. Mohebujjaman, "MHD heat and mass transfer free convection flow along a vertical stretching sheet in presence of magnetic field with heat generation," *Research Journal of Applied Sciences, Engineering and Technology*, vol. 1, no. 3, pp. 98–106, 2009.
[19] W. T. Kierkus, "An analysis of laminar free convection flow and heat transfer about an inclined isothermal plate," *International Journal of Heat and Mass Transfer*, vol. 11, no. 2, pp. 241–253, 1968.
[20] A. Aziz, "A similarity solution for laminar thermal boundary layer over a flat plate with a convective surface boundary condition," *Communications in Nonlinear Science and Numerical Simulation*, vol. 14, no. 4, pp. 1064–1068, 2009.